

Heat Treatment of Plasma Sprayed Hydroxyapatite Coatings: Microstructural and Mechanical Characterization

Vikas Rattan*¹, T. S. Sidhu², Manoj Mittal³

*¹Research Scholar, Inder Kumar Gujral Punjab Technical University, Kapurthala, Punjab, India

²Shaheed Bhagat Singh State Technical Campus, Ferozepur, Punjab, India

³Inder Kumar Gujral Punjab Technical University, Kapurthala, Punjab, India

ABSTRACT

In the present research, the emphasis has been laid to study the outcome of heat treatment on phases of hydroxyapatite in coatings developed by plasma spraying process. The surface morphology of as-deposited and heat treated HAp coated samples was studied using Scanning electron microscopy (SEM), X-ray diffraction analysis (XRD), and Fourier transformation infrared spectroscopy (FTIR) techniques. The results obtained by XRD analysis of the HAp coated samples after heat treatment reveal the formation of crystalline structure at 700°C with some traces of CaO. Moreover, when the heat treatment was further done at 900°C, the unwanted CaO was totally eliminated and coating with crystalline structure was obtained. Heat treatment reduces the surface roughness and porosity of the HAp coated samples.

Keywords: Hydroxyapatite, Heat Treatment, Plasma Spraying, AISI 304 L SS, Porosity, Crystallinity

I. INTRODUCTION

Hydroxyapatite [$\text{Ca}_{10}(\text{PO}_4)_6(\text{OH})_2$ (HAp)], is the crystalline phase of calcium phosphate and is a promising material for bone grafting and hard tissue replacement for bone and teeth. It has been broadly utilized as a covering material for implants in the form of granular, porous or dense forms. Due to its highly bioactive nature, chemical similarities, and crystalline structure prosthesis become stable within a very short period of time because apatite or the bone layer starts growing from the existing bone walls into the implant coated with hydroxyapatite which makes it biocompatible with the surrounding tissue [1-8].

Several methods are used to deposit HAp onto implant surfaces, such as thermal spraying (especially plasma spraying), sol-gel methods, electrophoretic deposition, sputter coating, hydrothermal method and hot isostatic pressing (HIP) [3-5, 9]. The Food and Drug Administration (FDA) of USA has allowed the plasma spraying process to be used for biomedical coating deposition because of its better coating characteristics as compared to other coating techniques [2, 3].

During the plasma spraying process, HAp powder is subjected to a very high temperature, which melts the powder to form coatings on the relatively cooled surface of the metallic implant. This results in the formation of unwanted phases like tricalcium phosphate, tetracalcium phosphate and calcium oxide. Bioactivity and crystallinity of hydroxyapatite coatings are greatly affected due to the occurrence of these phases. Change in composition of the coating as compared to powder residual stresses are developed in the coatings, which ultimately lead to the loosening of the implant [9-16]. For the long-term performance, stability, and safety of implant materials, HAp coatings with high crystallinity and fewer defects are desirable. HAp coatings with high crystallinity reduce the dissolution rate and enhance the cell growth [10, 17]. For improvement in crystallinity, proliferation rate and reduction in induced stresses heat treatment are used after the coating of hydroxyapatite onto the implant surface [18].

Lynn et al. [19] reported a reduction in fatigue resistance and recovery of the crystalline structure when heat treatment was done at 400°C for 90 h. The crystalline structure recovered was poorer to that observed with higher temperature treatments. The

literature had reported the reinstatement of crystalline structure and OH⁻ groups, when heat treatment at (600°C-700°C) for 2 h was done for the plasma sprayed HAp coatings [20]. Also, heat treatment at 600°C can maintain hydroxyl levels within the coatings and can attain the full crystallization of amorphous phase, minimal coating defects, and higher corrosion resistance [10, 18]. Some researchers, on the other hand, recommended that improvement in crystallinity and microstructure can be achieved when heat treatment is done at 760°C for 2h [11].

The present study has been focused on investigating the morphology, microstructure, and phase analysis of the HAp coatings and heat treated HAp coatings. The heat treatment of the coatings has been done at 700°C & 900°C temperature for a holding time of 2h. After heat treatment samples were cooled in the furnace for 12 hours or until the samples have attained the room temperature. The morphological, microstructural and phase analysis of HAp and heat treated coatings has been carried out using SEM/EDX, XRD, and FTIR techniques.

II. METHODS AND MATERIAL

2.1 Substrate material and deposition of coatings

Hydroxyapatite powder (Captal 60-1) with mean particle Size: $d(50) = 45.5 \mu\text{m}$, procured commercially from the Plasma Biotol Limited, UK has been used as the feedstock powder to develop coatings. SEM micrograph of the feedstock used for the plasma coating process is shown in Fig.1.

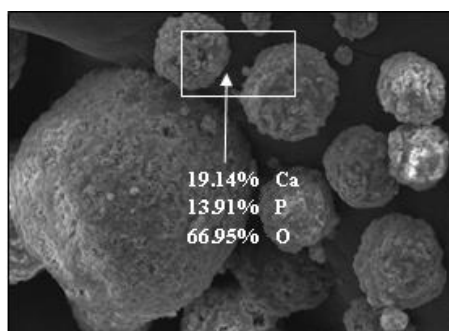


Figure 1: SEM micrograph and EDX analysis of HAp powder.

The AISI 304L SS has been used in the present study as the substrate material. The substrate material has been supplied by Steel Emporium, Mumbai, India in the form

of a rectangular strip having a thickness of 5mm. The actual chemical composition of the substrate material as presented in Table.1 has been determined with the help of Optical Emission Spectrometer (Foundry Master, Oxford- Instruments, England).

Table 1. Chemical composition (weight %) (actual and nominal) of AISI 304L SS

Elements	Nominal	Actual
C	0.03 Max	0.02
Si	1Max	0.33
Mn	2Max	1.29
P	0.045Max	0.020
S	0.03max	0.0091
Cr	18-20	17.7
Ni	8-12	8.52
Mo	2-3	0.23
Fe	Bal	Bal

The specimens for the present investigation were prepared by cutting the strip in dimensions 20 x 15 x 5 mm. Polishing of the uncoated substrate samples was done using emery papers of 180, 220, 400, 600 grades and later on 1/0, 2/0, 3/0, and 4/0 grades. The surface of the samples was made rough by grit blasting using alumina of grit size 60 μm and subsequently air blasted to remove any remaining alumina grit from the surface of the samples. The samples were then coated with hydroxyapatite using the plasma spraying apparatus (40 kW Miller thermal spray, USA) available at Anod Plasma Limited, Kanpur, India. The thickness of the coatings was monitored throughout the coating process and thickness in the range of 150-160 μm was finally obtained on the samples. The coating process parameters employed for plasma spraying are represented in the Table. 2.

Table 2 : Plasma spraying process parameters employed for coating the specimens

Process parameter	Value
Arc current (A)	500
Arc voltage (V)	50
Powder feed rate (g/min)	40
Standoff distance (mm)	100
Plasma arc gas pressure (psi)	60
Powder carrier gas pressure (psi)	45

2.2 Characterization of the coatings

SEM/EDX, XRD, and FTIR techniques have been utilized to characterize the morphology of the HAp powder, HAp coated specimens and HAp coated specimens after heat treatment. SEM/EDX analysis of the feedstock, HAp coated specimens and HAp coated specimens after heat treatment have been done with the help of a JEOL: JSM-6610LV scanning electron microscope (Japan) coupled with EDX attachment (Oxford-instruments, England). The feedstock powder, HAp coated specimens and HAp coated specimens after heat treatment, were also characterized with the help of XRD (Make: PANalytical, Model: X'pert Pro) using Cu K α radiation. A diffraction angle with a scan range of $2\theta = 10-90^\circ$ was used for the XRD analysis. The XRD patterns were analyzed using X'pert High Score (version 3.0) software. FTIR analysis has been done on FTIR spectrometer (Nicolet iS -10, USA). The IsoMet Precision Diamond Saw (Buehler, U.S.A) was used to cut the as coated specimens into proper sizes. The cut specimens were then hot mounted using the transoptic powder. The mounted specimens were mirror polished manually using emery papers of 400, 600, 800, 1000 and 1200 grades and later on 1/0, 2/0, 3/0, and 4/0 grades. The prepared samples were mirror polished using the 0.5 μ m alumina paste on the polishing machine. The surface porosity was measured with image analyzer based on standard test method (ASTM B276). The porosity images of the HAp coated and HAp coated specimens after heat treatment were obtained using an inverted metallurgical microscope (PMP3, Japan). The surface roughness of the HAp coated and HAp coated specimens after heat treatment were measured using the surface roughness tester (Mitutoyo SJ-201, Japan) using a Gaussian type filter for a cutoff length (λ_c) of 0.8mm. The surface roughness parameter R_a (average of the deviation of the roughness profile) has been used to represent the surface roughness of the as-deposited and heat-treated specimens. Surface roughness values represented here are the average of the five readings taken along different directions.

2.3 Post-coating Heat Treatment

The plasma sprayed samples of the HAp were heat treated in a digitally controlled furnace in an air environment to investigate the post-deposition heat treatment effects on the HAp coatings. The temperature of the furnace was set at 700°C and then at 900°C for a dwell time of 30 min for each temperature range. The

specimens were kept in a ceramic bowl and placed in the preheated furnace for a retention time of 2h. The specimens were permitted to cool in the furnace for minimum 12hour or until the room temperature has been reached. The cooled samples were then examined visually for the color change, cracks and peeling off from the surface of the samples.

III. RESULTS

3.1 Surface roughness and Porosity of the coatings

The surface roughness parameter (R_a) and porosity measurements for HAp coated and HAp coated specimens after heat treatment are represented in the Table.3.

Table 3. Porosity (% age) and surface roughness values (μ m) of HAp coated (as sprayed) and heat treated coatings

Specimens	Porosity (%age)	Surface Roughness (μ m)
Polished cross section	7.09 \pm 0.14	-----
As sprayed	6.71 \pm 0.16	6.27 \pm 1.4
Heat treated at 700°C	5.68 \pm 0.13	5.97 \pm 0.77
Heat treated at 900°C	5.99 \pm 0.19	5.91 \pm 0.05

The average surface roughness values for the mentioned specimens was found to be more for as coated specimens while the surface roughness decreases with the heat treatment. Also the porosity measurements carried out at different locations on the as coated and heat-treated specimens show that the porosity for the polished cross section is more and it decreases when measured for HAp coated and HAp coated specimens after heat treatment.

3.1 Surface morphology and Microstructure of coatings

The coating morphologies of HAp coated and HAp coated specimens after heat treatment at 700°C and 900°C are represented in Fig. 2. The SEM micrograph with EDX analysis of the HAp coated specimens on the AISI 304L is represented in Fig. 2 (a). The as-sprayed coating microstructure consists of some unmelted,

moderately melted and completely melted molten splats on its surface. The EDX analysis of the coatings demonstrates that the coatings are mainly formed of the elements Ca, P and O. Some minor cracks are also present along the coating surface. This may be caused due to the rapid cooling of the coating as compared to the substrate.

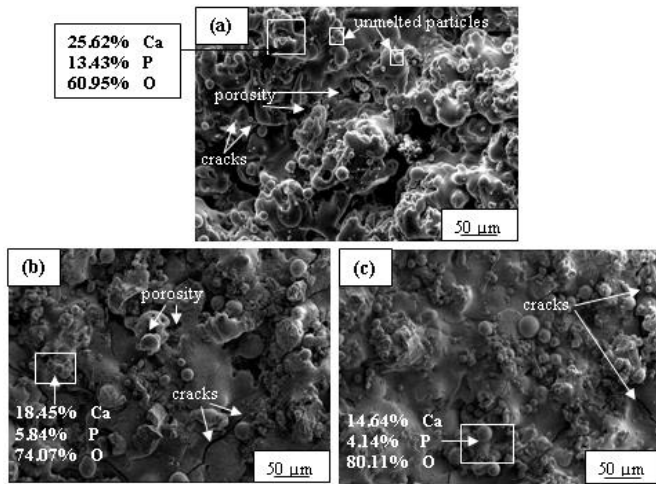


Figure 2: SEM micrographs and EDX analysis of plasma spray coating on AISI 304L SS (a) Pure HAP coatings, (b) heat-treated coatings at 700°C, (c) heat-treated coatings at 900°C

Fig. 2 (b-c) shows the SEM micrograph of the HAP coated specimens after heat treatment. The visual examination of the heat-treated coatings at 700°C and 900°C for 2h shows that the surface changes to the light green color which corresponds to the original color of the starting powder. The microstructure examination of heat-treated coatings show that the surface cracks present on the surface of the coatings opened and extended to a bigger size. In addition, the roughness of the coating increases after the heat treatment due to the formation of tiny particles on its surface.

3.3 Phase Analysis

Fig. 4 shows the XRD pattern obtained from coating powder, as deposited HAP coatings and heat-treated coatings at 700°C and 900°C.

Figure 4: X-ray diffraction patterns of (a) HAP powder, (b) As sprayed HAP coatings, (c) Heat-treated HAP coatings at 700°C, (d) Heat-treated HAP coatings at 900°C for 2 h in air. (Π : Pure HA, β : β -TCP, α : α -TCP, τ : TTCP, χ : CaO)

The XRD pattern, Fig. 4 (a) shows sharp peaks which correspond to pure HAP powder, indicating very high crystallinity of the powder. XRD analysis of the HAP coated specimens Fig. 4 (b) shows that the sharp peaks corresponding to HAP broaden after coating indicating the convergence of crystalline material to amorphous phase at approximately 30-33° on the XRD spectrum. The extra peaks most likely relate to the traces of α -TCP, β -TCP and TTCP. Fig. 4 (c-d) shows the XRD pattern for heat-treated coatings at 700°C and 900°C respectively. The intense, sharp peaks appeared when HAP coated specimens were heated at 700°C and 900°C. These sharp peaks correspond to the formation of the crystalline phase of the coating. However, very small traces of CaO were observed in the heat-treated coatings at 700°C, but it was completely eliminated when further heat-treated to 900°C.

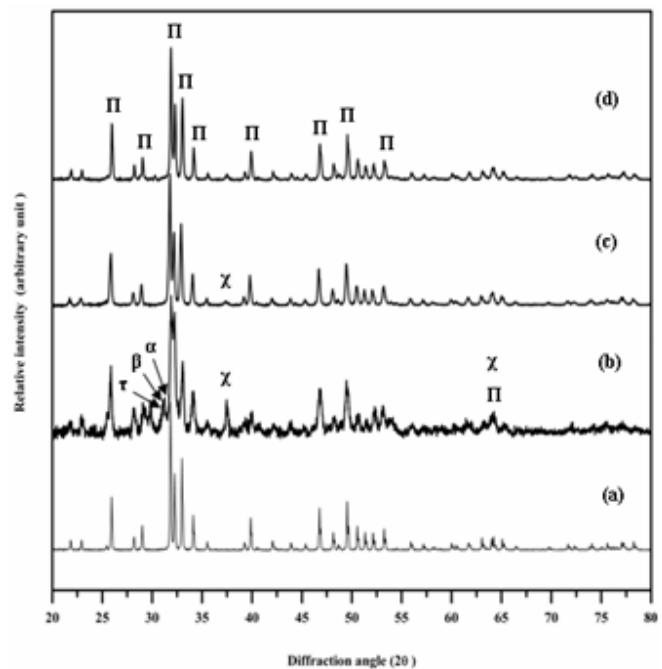


Figure 4.

The FTIR spectrum of the HAP powder, HAP coated specimens and HAP coated specimens after heat treatment at 700°C and 900°C, is shown in Fig.5.

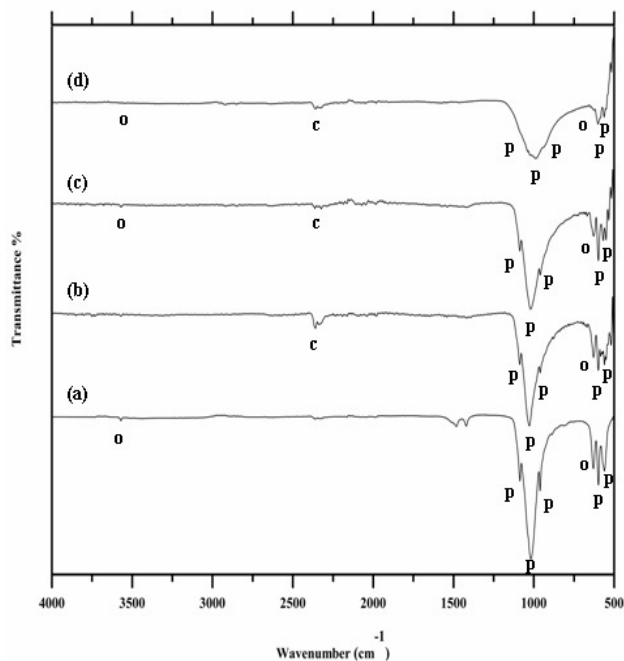


Figure 5. FTIR spectra of (a) HAp powder, (b) Pure HAp coatings, (c) Heat-treated HAp coatings at 700°C, (d) Heat-treated HAp coatings at 900°C: (o: OH⁻, c: CO₃⁻, p: PO₄³⁻).

The FTIR investigation of the HAp coated specimens and HAp coated specimens after heat treatment was carried out in the wavenumber range 4000 cm⁻¹ to 400 cm⁻¹. The presence of the OH⁻ group for pure HAp powder can be seen at 3573 cm⁻¹ and 627 cm⁻¹, whereas in the case of as-sprayed coatings these are at 3563 cm⁻¹ and 627 cm⁻¹. However, for heat-treated coatings at 700°C, the OH⁻ group is present at 3648 cm⁻¹ and 629 cm⁻¹, whereas it can be observed at 3569 cm⁻¹ when the coatings were heat treated at 900°C. The FTIR spectrum shows the presence of PO₄³⁻ group at 557 cm⁻¹, 596 cm⁻¹, 958 cm⁻¹, 1018 cm⁻¹ and 1086 cm⁻¹, in case of HAp powder, and at 559 cm⁻¹, 598 cm⁻¹, 627 cm⁻¹, 958 cm⁻¹, 1026 cm⁻¹ and 1086 cm⁻¹ in case of HAp coatings, whereas for heat-treated coatings at 700°C it is present at 567 cm⁻¹, 600 cm⁻¹, 960 cm⁻¹, 1024 cm⁻¹, and 1088 cm⁻¹. For heat-treated coatings at 900°C, PO₄³⁻ group can be observed at 563 cm⁻¹, 600 cm⁻¹, 980 cm⁻¹, 1024 cm⁻¹, and 1039 cm⁻¹.

IV. DISCUSSION

The HAp-coated AISI 304L stainless steel specimens have a uniform, dense microstructure having some minor cracks with the surface roughness of $R_a = 6.27 \pm 1.4 \mu\text{m}$ (for as-sprayed coatings), $R_a = 5.97 \pm 0.77 \mu\text{m}$ (for specimens heat-treated at 700°C) and $R_a = 5.91 \pm 0.05 \mu\text{m}$ (for specimens heat-treated at

900°C). The reduction in surface roughness of the specimens was attributed to the recrystallization of the HAp particles upon heat treatment. It has been reported that surface chemistry, crystallinity, and roughness play a significant purpose in cell binding, cell growth and quick response to cellular attachment [21]. Studies by L. Ponsonnet et al [22] demonstrates that cell expansion rate gets adversely affected if the roughness values exceed certain limits. Porosity being an important parameter is generally used to establish coating characteristics that are more mechanically strong and biocompatible [23]. In the present study, the apparent porosity of $7.09 \pm 0.14 \%$ for the polished cross section, $6.71 \pm 0.16 \%$ for as sprayed specimens, $5.68 \pm 0.13 \%$ for heat-treated specimens at 700°C and $5.99 \pm 0.19 \%$ for post coating heat-treated specimens at 900°C have been observed. The porosity was higher in the polished cross section specimens due to the removal of the coating particles while preparing samples. The porosity gets reduced as the heat treatment was performed on the coated specimens. This was due to the reason that the amorphous coating has been converted to crystalline that may have reduced the microstructural inhomogeneities due to the filling of the empty voids and pores. The as-sprayed coating is characterized by the presence of some moderately melted and totally melted powder particles. A few cracks are also visible on the surface of the coated specimens, which probably arise from residual stress upon rapid cooling and solidification [24]. The surface morphologies of HAp coatings and heat-treated coatings show no distinguishable differences [9, 10]. HAp coatings can be crystallized with the heat treatment process to additionally enhance the mechanical properties of coatings by reducing residual stresses, microcracks, and pores. There is no specific temperature at which amorphous HAp reverts to HAp with higher crystallinity but is a broader temperature zone [11]. Shinn et al [9] had reported that the convergence of amorphous phase to crystalline phase in the plasma sprayed coatings in the air could be effectively done at a temperature of 650°C. Heat treatment at this temperature range also reduces the flake type structure, which is usually associated with plasma sprayed coatings. The excessive holding time and high temperature are unfavorable for the structural integrity of HAp. The temperature of 600°C is favorable for the complete conversion of amorphous to a crystalline phase and to maintain hydroxyl levels within the coatings [18]. During the plasma spraying process, HAp

powder is subjected to very high temperatures, which readily melts the HAp powder. When the HAp molten particles strike the relatively cooled surface of the substrate microstructural changes occurs in the HAp during solidification. The elevated temperature and speedy cooling during the plasma spraying method lead to the formation of unfavorable phases like TCP, TTCP and CaO. These phases are readily soluble in the body fluids because of their amorphous structure, thus leading to loosening or instability of the implant [13]. Post-coating heat treatment is helpful to augment the mechanical properties, improve structural integrity and crystallinity and decrease residual stresses of HAp coatings [9, 11, 18]. The results of the XRD pattern of Fig. 4 shows the transformation of TCP, TTCP, and CaO present in HAp coatings and heat-treated coatings at 700°C to complete, crystalline HAp coatings when heat-treated at 900°C. The results are in close conformity with the previous results published [25, 26]. The FTIR spectra of the HAp powder, as deposited HAp coating and heat treated coating at 700°C and 900°C, are almost similar. No large variation in the spectra has been observed. It is clear from the FTIR spectra that at 2356 cm⁻¹, CO₃⁻ molecules were present in HAp coated specimens and HAp coated specimens after heat treatment which were not observed for HAp powder. The presence of CO₃⁻ molecules have been attributed to the absorbance of CO₂ from the atmosphere [27]. Good restoration of the sharp bond peak of OH approximately at wave numbers 3569 cm⁻¹ and 629 cm⁻¹ can be observed in heat-treated coatings only [18, 28].

V. CONCLUSIONS

Pure HAp coatings were successfully deposited onto the AISI 304L SS substrates by plasma spraying technique. HAp coatings exhibit some unmelted, partly melted, and completely melted particles of HAp with some minor cracks on its surface. The minor cracks arise from the localized stresses developed upon the cooling and solidification of the HAp coatings. The decomposition of hydroxyapatite powder due to the elevated temperature of plasma jet (approx. 300°C) results in the formation of unfavorable phases like α -TCP, β -TCP, TTCP and CaO phases. The SEM micrographs of the heat-treated HAp coatings reveal that the microstructure was not all differ from the as sprayed microstructure, except the cracks present on the coating surface widened after the heat treatment. The widening of

cracks can be attributed to the crystallization and hydroxylation of phases like α -TCP, β -TCP, TTCP and CaO. The contraction of hydroxyapatite coatings thus followed widens the cracks. Also, porosity and surface roughness of the HAp coatings reduces with the enhanced heat treatment temperature. As indicated by the XRD spectra of the heat treated coatings at 700°C, the amorphous phases almost disappear and the coating crystallinity was regained with some traces of CaO. Further, when the temperature was raised to 900°C the XRD peaks becomes sharper indicating the crystallinity of the HAp coatings without the CaO phase.

VI. ACKNOWLEDGEMENT

The author Vikas Rattan acknowledges Inder Kumar Gujral Punjab Technical University, Kapurthala, Punjab, India and Anod Plasma Limited, Kanpur, India for providing the amenities for carrying out this investigation.

VII. REFERENCES

- [1]. Porter AE., Patel N, and Best S., Hydroxyapatite. In: Wnek GE, Bowlin GL, editors. Encyclopedia of Biomaterials and Biomedical engineering. New York (NY): Informa Healthcare; 2008. p.145-1463
- [2]. Mittal M., Nath S K, and Prakash S., "Improvement in mechanical properties of plasma sprayed hydroxyapatite coatings by Al₂O₃ reinforcement", Material Science Eng C. ; Vol. 33(5), pp 2838-2845, 2013.
- [3]. Hasan M F., Wang J, and Berndt C C., "Effect of power and stand-off distance on plasma sprayed hydroxyapatite coatings", Materials and Manufacturing Processes. Vol. 28(12), pp1279-1285, 2013.
- [4]. S Yangyang., L Kezh., Z Leilei. Farhan S., Liu S, and Shi G., "Ca-P bioactive coating prepared by combining microwave-hydrothermal and supersonic atmospheric plasma spraying methods. Materials Science and Engineering C. Vol. 72, pp 371-377, 2017
- [5]. Sun R X., Liu P, Zhang X, Lv P Y, and Chen Z K., "Hydrothermal synthesis of microstructured fluoridated hydroxyapatite coating on magnesium alloy", Surface Engineering, Vol 32, pp 879-884, 2016.

- [6]. Wu S-C., Hsu H-C., Hsu S-K., Chang Y C, and Ho F W., "Effects of heat treatment on the synthesis of hydroxyapatite from eggshell powder", *Ceramics International*, Vol 41, pp 10718-10724, 2015.
- [7]. Singh G., Singh H, and Sidhu B S., "Corrosion behavior of plasma sprayed hydroxyapatite and hydroxyapatite-silicon oxide coatings on AISI 304 for biomedical application", *Applied Surface Science*, Vol 284, pp 811-818, 2013.
- [8]. Girardin E L., Hirschi K, and Lodini A., "Characterization techniques for hydroxyapatite deposited by plasma spray on hip prosthesis", *Materials and Manufacturing Processes*, Vol 13 (4), pp 581-588, 1998.
- [9]. Ding S J., Huang T H, and Kao C T., "Immersion behavior of plasma-sprayed modified hydroxyapatite coatings after heat treatment", *Surface and Coatings Technology*, Vol 165(3), pp 248-257, 2003.
- [10]. Chen C C, and Ding S J., "Effect of heat treatment on characteristics of plasma sprayed hydroxyapatite coatings", *Materials Transactions*, Vol 47, pp 935-940, 2006.
- [11]. Zhao G L., Wen G W, and Kun W., "Influence of processing parameters and heat treatment on phase composition and microstructure of plasma sprayed hydroxyapatite coatings", *Trans Nonferrous Met Soc China*, Vol 19, pp s463-s469, 2009.
- [12]. Tian Y S., Qian X L, and Chen M Q., "Effect of saturated steam treatment on the crystallinity of plasma-sprayed hydroxyapatite coatings", *Surface and Coatings Technology*, Vol 266, pp 38-41, 2015.
- [13]. Tian Y S., Qian X L, and Chen M Q., "Crystallinity improvement of hydroxyapatite coating by saturated steam treatment", *Surface Engineering*, Vol 31(1), pp 48-51, 2015.
- [14]. Kulpetchdara K., Limpichaipanit A., Rujijanagul G., randorn G, and Chokethawai K., "Influence of the nano hydroxyapatite powder on thermally sprayed HA coatings onto stainless steel", *Surface and Coatngs Technology*, Vol 306, pp 181-186, 2016.
- [15]. Vahabzadeh S., Roy M., Bandyopadhyay A, and Bose S., "Phase stability and biological property evaluation of plasma sprayed hydroxyapatite coatings for orthopedic and dental applications", *Acta Biomaterialia*, Vol 17, pp 47-55, 2015.
- [16]. Khodaei M., Meratian M., Shaltookhi M., Hashemibeni B., Savabi O, and Razavi M, "Surface modification of Ti6Al4 V implants by heat, H₂O₂ and alkali treatments", *Surface Engineering*, Vol 32(10), pp 786-793, 2016.
- [17]. Cao W, and Hench LL, "Bioactivematerials", *Ceramics International*, Vol 22, pp 493-507, 1996.
- [18]. Lu Y P., Song Y Z., Zhu R F., Li S M, and Li Q T, "Factors influencing phase compositions and structure of plasma sprayed hydroxyapatite coatings during heat treatment", *Applied Surface Science*, Vol 206, pp 345-354, 2003.
- [19]. Lynn A K, and DuQuesnay D L, "Hydroxyapatite-coated Ti-6Al-4V: Part 2: the effects of post-deposition heat treatment at low temperatures", *Biomaterials*, Vol 23, pp 1947-1953, 2002.
- [20]. Lu Y P, Li S T, Zhu R F, Li S M, and Li Q T, "Formation of ultrafine particles in heat treated plasma-sprayed hydroxyapatite coatings", *Surface and Coatings Technology*, Vol 165, pp 65-70, 2003.
- [21]. Deligianni D D., Katsala N D., Koutsoukos P G, and Missirlis Y F, "Effect of surface roughness of hydroxyapatite on human bone marrow cell adhesion, proliferation, differentiation, and detachment strength," *Biomaterials*, Vol 22, pp 87-96, 2000.
- [22]. Ponsonnet L., Reybier K., Jaffrezic N., Comte V, Lagneau C, Lissac M, and Martelet C, "Relationship between surface properties (roughness, wettability) of titanium and titanium alloys and cell behavior," *Materials Science and Engineering C*, Vol 23, pp 551-560, 2003.
- [23]. Mancini C E., Berndt C C, Sun L, and Kucuk A, "Porosity determinations in thermally sprayed hydroxyapatite coatings," *Journal of Materials Science*, Vol 36, pp 3891-3896, 2001.
- [24]. Khor KA., Yip CS, and Cheang P, "Ti-6Al-4V/hydroxyapatite composite coatings prepared by thermal spray techniques," *Journal of Thermal Spray Technology*, Vol 6(1), pp 109-115, 1997
- [25]. Xiao G Y., Lu Y P., Zhu RF., Li S-T, and Wang A-J, "Effect of post-deposition heat treatment on mechanical properties of thermally sprayed hydroxyapatite coating," *Surface Engineering*, Vol 24, pp 307-312, 2008
- [26]. Espanol M., Guipont V., Khor KA., Jeandin M, and Llorca-Isern N, "Effect of heat treatment on

high pressure plasma sprayed Hydroxyapatite coatings," Surface Engineerin, Vol 18, pp 213-218, 2002.

- [27]. Singh G., Singh S, and Prakash S, "Surface characterization of plasma sprayed pure and reinforced hydroxyapatite coating on Ti6Al4V alloy," Surface and Coatings Technology, Vol 205(20), pp 4814-4820, 2011.
- [28]. Mittal M., Prakash S, and Nath S K, "Recrystallization of amorphous phases via post-coating heat treatmentof plasma sprayed hydroxyapatite coatings,"Materials and Manufacturing Processes, Vol 27 (9) , pp 1001-1006, .2012.